IMMEDIATE COMMUNICATION

Discovery of a novel pseudo β-hairpin structure of N-truncated amyloid-β for use as a vaccine against Alzheimer's disease

Preeti Bakrania[1,7✉], Gareth Hall[2,7], Yvonne Bouter[3,7], Caroline Bouter[4], Nicola Beindorff[5], Richard Cowan[2], Sarah Davies[1], Jemma Price[1], Chido Mpamhanga[1], Elizabeth Love[1], David Matthews[1,6], Mark D. Carr[2✉] and Thomas A. Bayer[3✉]

One of the hallmarks of Alzheimer's disease (AD) are deposits of amyloid-beta (Aβ) protein in amyloid plaques in the brain. The Aβ peptide exists in several forms, including full-length Aβ1-42 and Aβ1-40 – and the N-truncated species, pyroglutamate Aβ3-42 and Aβ4-42, which appear to play a major role in neurodegeneration. We previously identified a murine antibody (TAP01), which binds specifically to soluble, non-plaque N-truncated Aβ species. By solving crystal structures for TAP01 family antibodies bound to pyroglutamate Aβ3-14, we identified a novel pseudo β-hairpin structure in the N-terminal region of Aβ and show that this underpins its unique binding properties. We engineered a stabilised cyclic form of Aβ1-14 (N-Truncated Amyloid Peptide AntibodieS; the 'TAPAS' vaccine) and showed that this adopts the same 3-dimensional conformation as the native sequence when bound to TAP01. Active immunisation of two mouse models of AD with the TAPAS vaccine led to a striking reduction in amyloid-plaque formation, a rescue of brain glucose metabolism, a stabilisation in neuron loss, and a rescue of memory deficiencies. Treating both models with the humanised version of the TAP01 antibody had similar positive effects. Here we report the discovery of a unique conformational epitope in the N-terminal region of Aβ, which offers new routes for active and passive immunisation against AD.

Molecular Psychiatry (2022) 27:840–848; https://doi.org/10.1038/s41380-021-01385-7

INTRODUCTION

Alzheimer's disease (AD) is a progressive neurodegenerative condition characterised by the presence of extracellular deposits of the amyloid-beta (Aβ) protein. While amyloid plaques represent typical hallmarks of AD, soluble oligomers have been shown to better correlate with the clinical pathology [1]. Growing evidence suggests that soluble forms of Aβ are key to AD progression and may represent attractive therapeutic targets as they inhibit long-term potentiation, trigger synaptic plasticity and synapse loss [2–4]. A number of major variants of extracellular Aβ have been identified, including full-length Aβ1-42, Aβ1-40, Aβ4-42 and a form with an N-terminal pyroglutamate (pE, pGlu) Aβ3-42 (AβpE3-42) [5, 6]. N-truncated Aβ species are highly abundant in AD brain [7], are toxic and induce synaptic dysfunction [5, 6, 8, 9]. Passive immunisation with TAP01, a murine antibody directed against the N-terminus of AβpE3-42 has beneficial effects in preclinical AD mouse models [10].

The "amyloid cascade hypothesis" claims that assemblies of monomeric Aβ initiate a process leading to neuron dysfunction, neuron death and dementia [11]. The most toxic forms of Aβ assemblies are soluble oligomers rather than fibrillary assemblies [12, 13]. Dimeric oligomers extracted from AD brain impaired synaptic structure and function [2]. Ono et al. [14] reported that Aβ monomers are unstructured, but oligomers exhibit order-dependent increases in β-sheet content. The authors used electron microscopy and atomic force microscopy to show that dimerisation and subsequent monomer addition are processes in which significant and asymmetric monomer conformational changes occur.

Solid-state nuclear magnetic resonance and electron microscopy studies by Chimon et al. [15] have led to the proposal that before fibrillisation, natively unstructured monomeric Aβ is subject to large conformational changes involving predominantly β-sheet type structures. Kayed et al. [16] discovered that soluble oligomers are common to amyloids, like the Aβ peptide in AD and demonstrated that the soluble amyloid oligomers tested display a common conformation-dependent structure unique to soluble oligomers regardless of the primary sequence. Moreover, oligomer-specific antibodies were found to recognise soluble oligomers derived from a diverse range of proteins, including insulin, α-synuclein and prion protein and neutralised their toxicity in vitro.

Here, we report that TAP01 family antibodies uniquely bind to a novel, pseudo β-hairpin conformation of the N-terminal region of Aβ, which is not related to any other Aβ epitope, conformation or aggregate structure described so far. A structure solved for TAP01

[1]LifeArc, Centre for Therapeutics Discovery, Open Innovation Campus, Stevenage, UK. [2]Leicester Institute of Structural and Chemical Biology and Department of Molecular and Cell Biology, Henry Wellcome Building, University of Leicester, Leicester, UK. [3]Department of Psychiatry and Psychotherapy, University Medical Center Göttingen (UMG), Georg-August-University, Göttingen, Germany. [4]Department of Nuclear Medicine, University Medical Center Göttingen (UMG), Georg-August-University, Göttingen, Germany. [5]Berlin Experimental Radionuclide Imaging Center (BERIC), Charité-Universitätsmedizin Berlin, Berlin, Germany. [6]Present address: Mogrify, Bio-Innovation Centre, Cambridge Science Park, Cambridge, UK. [7]These authors contributed equally: Preeti Bakrania, Gareth Hall, Yvonne Bouter. ✉email: Preeti.Bakrania@lifearc.org; mdc12@leicester.ac.uk; tbayer@gwdg.de

Received: 14 July 2021 Revised: 16 October 2021 Accepted: 27 October 2021
Published online: 15 November 2021

in complex with AβpE3-14 guided the design of a cyclised form of Aβ1-14 to stabilise the pseudo β-hairpin conformation in solution. Studies in two established mouse models of AD (5XFAD [17] and Tg4-42 [18]) showed substantial therapeutic benefits from either active immunisation with cyclised Aβ1-14 or passive immunisation with a humanised variant of TAP01, which reveals two attractive new options for AD treatment, including a potentially transformative vaccination approach.

MATERIAL AND METHODS

Preparation of cyclised Aβ peptides

Thioacetal cyclised peptides of Aβ1-14 were designed by LifeArc and Leicester, with synthesis and purification carried out by Cambridge Research Biochemicals.

ELISA assays of TAP01 family antibodies binding to Aβ peptides

ELISA antibody binding assays were carried out using standard protocols with a selection of Aβ peptides immobilised by biotinylation for the cyclised Aβ1-14, or by direct coating on plates for Aβ1-42, pE3-42 and 4-42. Briefly, Aβ peptides were coated on to 384 well plates, blocked, incubated with TAP01 family antibodies for 1 hr at 37 °C, and secondary-HRP conjugated antibodies were added, incubated for 1 hr at 37 °C. Plates were developed using K-BLUE substrate (20ul/well) and RED-STOP (10ul/well) solution. Optical density at 650 nm was measured using the Pherastar Plus.

Protein expression and purification for crystallography studies

The Fab fragments for the TAP01 family antibodies was cloned into LifeArc's in house LIC vectors, expressed in Expi293 cells for 5 days and cell culture supernatants processed for purification. Fab fragments were purified using a 2-step protocol, affinity chromatography followed by size exclusion chromatography (SEC). Purified AβpE3-14 and cyclised Aβ1-14 were solubilised in 25 mM Tris-HCl (pH 7.5) and 50 mM NaCl to 1 mM. The TAP01 (and other TAP01 family antibodies) complexes with N-terminal Aβ peptides were produced by mixing a 1.5 fold molar excess of peptide with antibody in a 25 mM Tris-HCl (pH 7.5) and 50 mM NaCl buffer followed by concentration of the complexes to ~14 mg/ml for crystallisation trials.

Crystallisation and structure determination of TAP01 family antibodies bound to Aβ

All crystals of Fab-Aβ peptide complexes were obtained by the vapour diffusion method at 19 °C, by mixing equal volumes of protein plus well solution. The TAP01-AβpE3-14 crystals grew in 20% PEG3350 and 0.2 M ammonium citrate. TAP01-cyclised Aβ1-14 crystals grew in 20% PEG 6 K, 0.1 M HEPES, pH 7.0, and 0.01 M zinc chloride. For cryoprotection, crystals were generally transferred to a solution of mother liquor plus 22% ethylene glycol. Data sets were collected at the European Synchrotron Radiation Facility (beamline ID30B (TAP01-AβpE3-14)) or at diamond light source (beamline I04 (TAP01-cyclised Aβ1-14)). Co-crystals of TAP01 with AβpE3-14 were refined to 1.4 Å resolution, whereas TAP01 with bound cyclised Aβ1-14 was refined to 2.5 Å. Data were processed using XDS [19] and AIMLESS from the CCP4 [20]. Both complex crystal struct ures were solved by molecular replacement using Phaser [21] using a homology model for the TAP01 antibody generated using SWISSMODEL [22] to model the heavy and light chains. Atomic models were built using Coot [23] and refined with Refmac [24], Phenix [25] and PDB_REDO [26]. The refinement statistics for both structures are summarised in Supplemental Table 1. The coordinates for the TAP01-AβpE3-14 and TAP01-cyclised Aβ1-14 peptide have been deposited to the PDB and given the codes 7OW1 and 7OXN, respectively.

Human specimens

The brains of 22 sporadic female AD patients (mean age 78.9 ± 2.1 SEM; Braak stage 4–6; ApoE4: 17/35) and five non-demented control patients (1 female/4 males, mean age 81.0 ± 4.6 SEM; Braak stage 0–1) were analysed. All human cortical brain samples were obtained from the Netherlands Brain Bank (NBB, Amsterdam, Netherlands). The use of human material was approved by the local ethical committee.

Alzheimer's disease mouse models

Two established Alzheimer's disease mouse models were used in the work reported here. Tg4-42 mice express human Aβ4-42 under the control of the neuronal Thy-1 promoter [18]. 5XFAD mice overexpress the 695 amino acid isoform of the human amyloid precursor protein (APP695) carrying the Swedish, London and Florida mutations under the control of the murine Thy1-promoter. In addition, human presenilin-1 (PSEN-1) carrying the M146L/L286V mutations is expressed under the control of the murine Thy1-promoter [17]. Full-length Aβ1-42 represents the by far the dominant fraction in 5XFAD mouse brain, whereas AβpE3-42 and Aβ4-42 are only minor fractions [27]. 5XFAD mice used in the current study were backcrossed for more than ten generations to C57Bl/6 J wildtype mice (Jackson Laboratories, Bar Harbor, ME, USA) to obtain an incipient congenic line on a C57Bl/6 J genetic background [28]. Tg4-42 mice were generated and kept on a C57Bl/6 J genetic background.

Immunohistochemical staining of paraffin sections of mouse brain samples

Mice were transcardially perfused with 4% paraformaldehyde in phosphate-buffered saline. Brain samples were carefully dissected and post-fixed in 4% phosphate-buffered formalin at 4 °C. The following antibodies were used: polyclonal antisera M2 derived from the active immunisation of wildtype mice (1:500), polyclonal antibody 24311, monoclonal antibody 1-57 against pyroglutamate Aβ3-X [29], Synaptic Sytems (Göttingen, Germany; 1 mg/ml; 1:500), solanezumab (cloned into mouse IgG1; 1:2500; 1.5 mg/ml) and TAP01_04 (1:200; 2 mg/ml). Corresponding biotinylated secondary antibodies (1:200) were purchased from DAKO (Glostrup, Denmark). Staining was visualised using the ABC method, with a Vectastain kit (Vector Laboratories, Burlingame, USA) and diaminobenzidine (DAB) as chromogen. Counterstaining was carried out with hematoxylin.

Quantification of Aβ load in human brain samples

Plaque load was quantified as previously described [10]. 5–6 paraffin embedded sections, which were at least 40 µm apart from each other, were stained simultaneously with DAB as chromogen. For thioflavin S fluorescent staining tissue sections were deparaffinised and rehydrated, washed twice in deionized water and then treated with 1% (w/v) thioflavin S in aqueous solution and counterstained in a 1% (w/v) aqueous solution of 4´6-diamidin-2-phenylindol. The relative Aβ load was evaluated using an Olympus BX-51 microscope equipped with an Olympus DP-50 camera and the ImageJ software (NIH, USA). Representative pictures of 20× magnification were systematically captured. Using ImageJ the pictures were binarised to 8-bit black and white pictures and a fixed intensity threshold was applied defining the DAB staining. Measurements were performed for a percentage area covered by DAB staining, as well as for the number of grains per mm^2 and the average size of the grains.

Spatial reference memory assessment by the Morris water maze

Spatial reference memory in mice was evaluated using the Morris water maze [30].

Quantification of neuron numbers using unbiased stereology

Stereological analysis was performed as previously described [28]. The hippocampal cell layer CA1 (Bregma −1.22 to −3.52 mm) was delineated on cresyl violet-stained sections and analysed with a stereology workstation (Olympus BX51 with a motorised specimen stage for automatic sampling), StereoInvestigator 7 (MicroBrightField, Williston, USA) and a 100x oil lens (NA = 1.35).

Active immunisation of mice with a cyclised Aβ1-14 peptide

Immunisation of wild-type mice with the cyclised Aβ1-14 was performed by David's Technologies using standard procedures. Addavax (Invivogen) was used as the adjuvant and immunisations performed using a 63 day protocol (5 x 75 ug antigen injected per mouse). 5XFAD or Tg4-42 mice were immunised starting at 8 weeks of age with the cyclised Aβ1-14 peptide [thioacetal bridged Aβ peptide 1-14 – KLH conjugate; DAC*FRHDSGYEC*HH[Cys]-amide (*S-CH-S bridged)] emulsified in complete Freund's adjuvant (CFA), followed by booster doses of protein emulsified in incomplete Freund's adjuvant (IFA). In 5XFAD mice booster injections of antigen emulsified in IFA were administered at day 14, day 28, day 42 and

10 weeks after the first immunisation dose. Similarly, in Tg4-42 mice booster injections of antigen emulsified in IFA were administered at day 14, day 28, day 42 and thereafter monthly (3 times after month 4, 5 and 6) following the first immunisation dose. The mice were injected with the cyclised Aβ1-14 peptide emulsified in CFA or IFA subcutaneously at two sites on the back, injecting 0.05–0.1 mL at each site (total of 0.1–0.2 mg per mouse). The boosters were given as single subcutaneous injections of 0.1 mL of IFA emulsion at one site on the back. Serum samples were isolated after sacrifice of the mice for titre determination (Fig. S1).

Passive immunisation of mice by treatment with TAP01 family antibodies

Passive immunisation was performed as previously described [10] by intraperitoneal injections of TAP01 family antibodies and an isotype control immunoglobulin. Mice were immunised by injections of the antibodies at a dose of 10 mg/kg body weight, diluted in sterile PBS (pH 7.4). 5XFAD mice received weekly injections beginning at 6 weeks of age, whereas Tg4-42 was started later at 3 months of age due to different onset of pathology in these mouse lines. Each mouse received a total of 12 injections. Behaviour testing in Tg4-42 started between the ninth and the tenth injection. Animals were sacrificed after the last injection (Fig. S2).

^{18}F-FDG-PET/MRI of glucose metabolism in mouse brains

^{18}F-FDG-PET was performed on mice essentially as previously described [31]. Mice were fasted overnight and blood glucose levels were measured before tracer injection. 15–22 MBq (mean 18.83 MBq) ^{18}F-FDG was injected intravenously into a tail vein with a maximum volume of 200 µl followed by an uptake period of 45 min. Mice were awake during the uptake process. PET scans were performed for 20 min using a small animal 1 Tesla nanoScan PET/MRI (Mediso, Hungary). Mice were anesthetised with isoflurane supplemented with oxygen during the scans and kept on a heated bed (37 °C). Respiratory rate was measured throughout the imaging process. MRI-based attenuation correction was conducted with the material map (matrix 144 × 144 x 163 with a voxel size of 0.5 × 0.5 × 0.6 mm^3) and the ^{18}F-FDG-PET images were reconstructed using the following parameters: matrix 136 × 131 x 315, voxel size 0.23 × 0.3 × 0.3 mm^3.

^{18}F-florbetaben-PET/MRI of for amyloid-plaque load in mouse brains

^{18}F-florbetaben-PET/MRI was performed on mice using 11–22 MBq (mean 16.23 MBq) of ^{18}F-florbetaben (Life Radiopharma Berlin GmbH, Germany) was administered intravenously into a tail vein with a maximum volume of 200 µl [32]. PET acquisition of 30 min duration started after an uptake period of 40 min. MRI-based attenuation correction was conducted with the material map, and the PET images were reconstructed as described above for ^{18}F-FDG-PET/MRI.

PET-image analysis

All PET images were analysed using PMOD v3.9 (PMOD Technologies, Switzerland) as described before [33]. A predefined MRI-based mouse brain atlas template was used to define different volumes of interest (VOIs). PET VOI statistics (kBq/cc) were generated for all brain areas and standardised uptake values (SUVs) were calculated as follows [SUV = tissue activity concentration average (kBq/cc) x body weight (g)/ injected dose (kBq)] for semi-quantitative analysis. SUVs of ^{18}F-FDG-PET scans were corrected for measured blood glucose levels as follows [SUVGlc = SUV x blood glucose level (mg/dl)]. SUVs of ^{18}F-florbetaben scans were normalised by SUVs taken from the cerebellum VOI and obtained ratios (SUVr) were used for further analysis.

Statistical analysis

The statistical significance of differences between groups of mice were tested with either one-way analysis of variance (ANOVA) followed by Bonferroni multiple comparisons, ANOVA followed by t-test, or two-way repeated measures ANOVA, as indicated. All appropriate data are reported as the mean with either standard error of the mean (SEM), or standard deviation (SD), as indicated. Significance levels are given as follows: ****$p < 0.0001$; ***$p < 0.001$; **$p < 0.01$; *$p < 0.05$. All statistics were calculated using GraphPad Prism version 8 for Windows (GraphPad Software, San Diego, CA, USA).

Study approval of animal experiments

All animal experiments reported here were approved by the local animal protection authorities Niedersächisches Landesamt für Verbraucherschutz und Lebensmittelsicherheit (LAVES, 26029 Oldenburg, Germany, approval number 17/2447) and Landesamt für Gesundheit und Soziales (LAGeSo, 10589 Berlin, Germany, approval number G0260/19). The experiments were conducted in accordance with the approved protocols.

RESULTS

TAP01 identifies a distinctive conformational Aβ epitope

Our hypothesis is that N-terminal truncated Aβ is a significant factor driving the pathology of AD. To that end, we embarked on a programme of work to identify novel therapeutics to target N-truncated Aβ. We have previously reported the identification of a novel murine antibody TAP01. The antibody was selected on the basis of two criteria: it should only bind N-truncated AβpE3-42 and Aβ4-42 but not Aβ1-42 and additionally the antibody must only bind low molecular weight Aβ [10, 34]. Here, we demonstrate that the humanised form of TAP01, TAP01_04 (Fig. S3) retains these properties. Moreover, it also offers protection in passive immunisation in the 5XFAD and Tg4-42 models of AD. In order to better understand the mechanism of action of TAP01 family antibodies we undertook a series of structural studies.

Identification of a unique Aβ conformational epitope and stabilisation by design of a cyclised form of Aβ 1-14

The pE3-42 and 4-42 forms of Aβ were found to rapidly aggregate in solution and were not amenable to the preparation of antibody-bound Aβ complexes for protein crystallography. In contrast, antibody Fab complexes of TAP01 formed with AβpE3-14 produced crystals that diffracted to 1.4 Å. The structure of the TAP01 Fab AβpE3-14 complex was solved by molecular replacement using a homology model of the antibody Fab fragment (Fig. 1). After placement of the antibody component of the complex, unambiguous additional density for the bound AβpE3-14 peptide was observed at the conventional antigen binding surface on TAP01, permitting the modelling of Aβ residues pGlu3-Val12 (Fig. 1A). Importantly, this revealed a novel pseudo β-hairpin conformation for the N-terminal region of Aβ bound to TAP01 (Fig. 1B), which is clearly present in solution for recognition by the antibody but has not been identified previously. The pseudo β-hairpin region of Aβ contains an isolated 5-residue α-turn, with the sequence Arg5-His-Asp-Ser-Gly9, which is further stabilised by a salt bridge between the guanidinium group of Arg5 and the carboxyl side chain of Asp7. With the exception of CDR-L2, at least one residue from all the CDR loops of TAP01 is within 5 Å of AβpE3-14, with 15 CDR residues losing at least 10 Å^2 of solvent accessibility on Aβ binding and making direct contacts with the peptide. The TAP01-AβpE3-14 interface features a mixture of polar and hydrophobic contacts, including the involvement of five aromatic side chains in CDRs from both the V_H (Tyr32, Trp52, Tyr101) and V_K (Tyr32 and Tyr36) domains (Fig. 1C).

The close proximity of the N- and C-termini of TAP01-bound AβpE3-14 enabled the design of cyclised forms of Aβ1-14, in which residues Glu3 and Val12 were replaced by cysteine and connected by a thioacetal bridge to stabilise the pseudo β-hairpin conformation of this region of Aβ. The structure of cyclised Aβ1-14 [thioacetal bridged Aβ peptide 1-14 – KLH conjugate; DAC*FRHDS-GYEC*HH[Cys]-amide (*S-CH-S bridged)] bound to TAP01 Fab was solved by protein crystallography to 2.5 Å resolution and showed that the cyclised peptide adopts the same conformation as native pE3-14 (Fig. 1D). A Cα alignment of cyclised Aβ1-14 with native AβpE3-14 gives an overall R.M.S.D. of ~0.5 Å. Whilst a number of reported antibodies are able to bind to AβpE3-42, TAP01 and humanised variants such as TAP01_04 were the only antibodies found to recognise and bind the novel pseudo β-hairpin conformation of Aβ reported here (Fig. S4), which underpins the

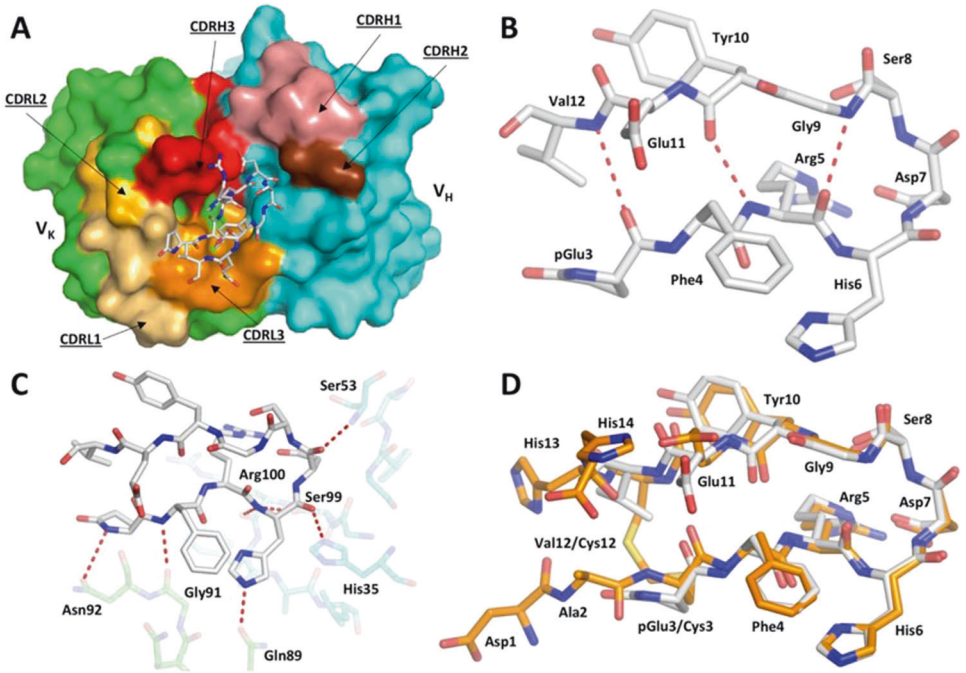

Fig. 1 Structure of the TAP01-Aβ pE3-14 complex. A A surface representation of the TAP01 antibody paratope, with the V_H and V_K domains coloured cyan and green respectively, and the individual complementary determining regions (CDR) highlighted. The conformation and location of the bound AβpE3-14 peptide is shown as a white sticks representation of its covalent structure. **B** The striking pseudo β-hairpin conformation of the TAP01 bound pE3-14 peptide, which is shown as a covalent sticks representation with stabilising intramolecular hydrogen bonds highlighted. **C** A detailed view of the TAP01-AβpE3-14 interface, with the bound peptide and interacting antibody residues shown as covalent sticks. TAP01 residues are shown in cyan and green for the V_H and V_K domains, respectively. Intermolecular hydrogen bonds between AβpE3-14 and the antibody are highlighted by dashed lines. **D** An overlay of the highly similar TAP01-bound conformations seen for cyclised Aβ1-14 and AβpE3-14, which are shown as orange and white covalent sticks, respectively.

unique functional affects and AD therapeutic potential of TAP01 family of antibodies. This also implies a key functional role for the pseudo β-hairpin conformation of the N-terminus of Aβ in driving AD progression and/or onset. The lack of binding of bapineuzumab, solanezumab, BAN2401, donanemab, ProBioDrug 6-1-6 and ProBioDrug 24-2-3 to Aβ1-14 containing a pseudo β-hairpin structure confirms the unique conformational epitope recognised by TAP01 family antibodies.

Active immunisation with cyclic Aβ 1-14 peptide raised a pseudo β-hairpin-specific Aβ antibody response

The identification of a pseudo β-hairpin structure as one preferred conformation for the N-terminal region of Aβ was completely unexpected and had not been suggested previously. Our work reported here and previously [10] strongly suggests that this conformation of Aβ exists naturally in solution and is a key driver of AD pathology. Antisera obtained from wildtype mice after active immunisation with the cyclised Aβ1-14 peptide revealed high levels of serum immunoglobulins (Fig. S5). The binding to cyclic Aβ1-14 was highest with 1/72.900 for sera of mouse M2 and 1/24.300 for mouse M4. The binding to 1-42 (M2: 1/8.100; M4: 1/2.700), to pE3-42 (M2: 1/2.700; M4: 1/2.700) and 4-42 (M2: 1/100; M4: 1/100) was significantly lower. Antisera obtained from 5XFAD and Tg4-42 mice after active immunisation with the cyclised Aβ1-14 peptide revealed high levels of serum immunoglobulins that bind to cyclised Aβ1-14 (Fig. S6) and to a lesser extent to Aβ1-42, AβpE3-42, Aβ4-42 (Fig. S7). Importantly, TAP01 family antibodies that uniquely recognise this pseudo β-hairpin conformation are protective in AD animal models and furthermore do not interact with fibrillary forms of amyloid typically seen in plaques of AD brain sections (Fig. S8). This exciting finding reveals new opportunities for AD therapeutic intervention, with options for both therapeutic TAP01 family antibodies and vaccine development. To explore the potential of an innovative vaccine approach to AD we undertook a series of animal studies to determine if immunisation with a stabilised pseudo β-hairpin form of Aβ1-14 showed any protection in mouse models of AD and to compare potential beneficial affects to treatment with the humanised TAP01_04 antibody.

In vivo imaging of immunised 5XFAD mouse brains shows a reduction of plaque load and a rescue of cerebral glucose metabolism

Active immunisation with cyclised Aβ1-14 peptide demonstrated significant beneficial effects on in vivo amyloid plaque load using the amyloid tracer tracer ^{18}F-florbetaben and assessing the retention signalling by positron emission tomography (PET) magnetic resonance imaging (MRI) (Fig. 2A–O), as well as comparable reductions in amyloid load revealed by immunostaining of brain sections (Fig. S9) of 5XFAD mice. Significantly lower amyloid-specific tracer ^{18}F-florbetaben retention signals were observed in the cortex, hippocampus, thalamus, forebrain, amygdala, olfactory bulb and midbrain (Fig. 2P). This was supported by quantification of the cortical plaque load using antibodies against pan-Aβ, AβpE3-X, Aβ4-X and staining against fibrillary amyloid (Fig. S9). The beneficial treatment effect achieved by active immunisation with cyclised Aβ1-14 and by passive immunisation with TAP01_04 antibody was similar across these imaging investigations, which clearly suggests that both approaches target the pseudo β-hairpin conformation of Aβ (Fig. 2).

Active immunisation with the cyclised Aβ1-14 peptide was also studied by in vivo glucose PET, which provides a clinically relevant assessment of the potential of the vaccine approach for AD treatment and prevention. ^{18}F-fluorodesoxyglucose (^{18}F-FDG) is an imaging biomarker that allows the analysis of cerebral glucose

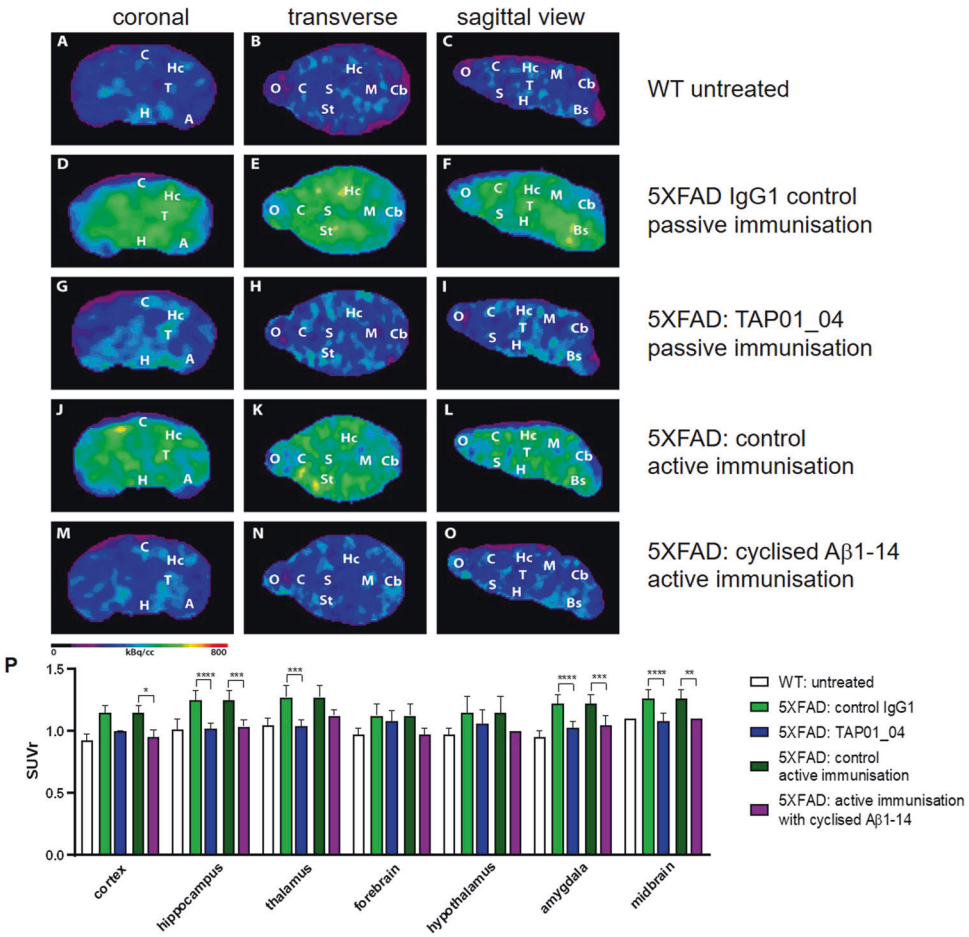

Fig. 2 Active and passive immunisation reduced amyloid plaque load in 5XFAD mice. PET images with amyloid-plaque tracer florbetaben reveal a reduction in plaque load induced by either active immunisation with cyclised Aβ1-14 or treatment with the antibody TAP01_04 (passive immunisation). PET images (coronal, transverse and sagittal views) were obtained from untreated WT ($n = 4$) and active or passive immunised 5XFAD mice, with appropriate controls ($n = 5$ each group). **A–C** PET images of WT mice. **D–F** PET images of 5XFAD mice after passive immunisation with an isotype control antibody. **G–I**. PET images of 5XFAD mice after passive immunisation with TAP01_04. **J–L** PET images of 5XFAD mice following control active immunisation. **M–O** PET images of 5XFAD mice after active immunisation with the cyclized Aβ1-14 peptide. **P** Quantitative analysis showed lower signals in different brain areas. Abbreviations: WT wild-type, A amygdala, Bs brain stem, C cortex, Cb Ccrebellum, H hypothalamus, Hc hippocampus, M midbrain, O olfactory bulb, S septum/basal forebrain, St striatum, T thalamus. Statistical analysis of the PET retention signal intensities was carried out by one-way ANOVA with Bonferroni multiple comparisons ($F = 14.28$, $p < 0.0001$, R squared 0.7361). The quantitative data are presented as mean ± S.E.M; ****$p < 0.0001$; ***$p < 0.001$; **$p < 0.01$; *$p < 0.05$.

metabolism in vivo using ^{18}F-FDG-PET, which is an established method for clinical diagnosis of AD in patients [34] and of neuronal dysfunction in AD mouse models including 5XFAD [33]. We observed significant beneficial effects of active immunisation with cyclised Aβ1-14 on glucose metabolism in 5XFAD mice, with a substantial rescue of levels of ^{18}F-FDG uptake in the cortex, hippocampus, thalamus, forebrain and midbrain (Fig. 3).

Immunised Tg4-42 mice retain cognitive function and neuron numbers in the hippocampus

It is well established that glucose consumption in the brain is a reliable indicator of normal functioning of synapses and neurons; hence, the positive effects assessed by ^{18}F-FDG-PET in 5XFAD mice induced by active immunisation with cyclised Aβ1-14 may be beneficial for memory and cognition in AD patients. In order to test a potential beneficial effect on neuron death and memory, we performed active immunisation with the cyclised Aβ1-14 peptide in Tg4-42 mice and compared the outcomes with passive immunisation with the TAP01_04 antibody. Stereological counting of CA1 neurons in the hippocampus, which are known to be primarily affected and degenerated in the Tg4-42 mouse model, revealed that both active and passive immunisation significantly prevented neuron death (Fig. 4A). This was supported by assessing hippocampus-dependent learning and memory in this model [35]. After immunisation of Tg4-42 mice a significant improvement in their ability to find the hidden platform in the probe trial of the Morris water maze was observed (Fig. 4B, Movie S1). Again, both active and passive immunisations elicited similar beneficial effects.

DISCUSSION

The groundbreaking work by Schenk et al. [36] clearly demonstrated that active immunisation with full-length aggregated Aβ1-42 significantly cleared plaques in an AD mouse model. Shortly afterwards, this concept was translated in a phase I immunotherapy trial in patients with mild to moderate AD using the vaccine AN1792 (human aggregated Aβ1-42) [37]. The follow-up phase IIa trial was prematurely terminated because of meningoencephalitis in 6% of immunised patients [38]. Post-mortem neuropathological examination of a group of AN1792 immunised AD patients verified clearance of amyloid plaques; however, this clearance did not prevent progressive neurodegeneration [39]. A lower plaque load, reduced tau load in neuronal processes, but not in cell bodies; and

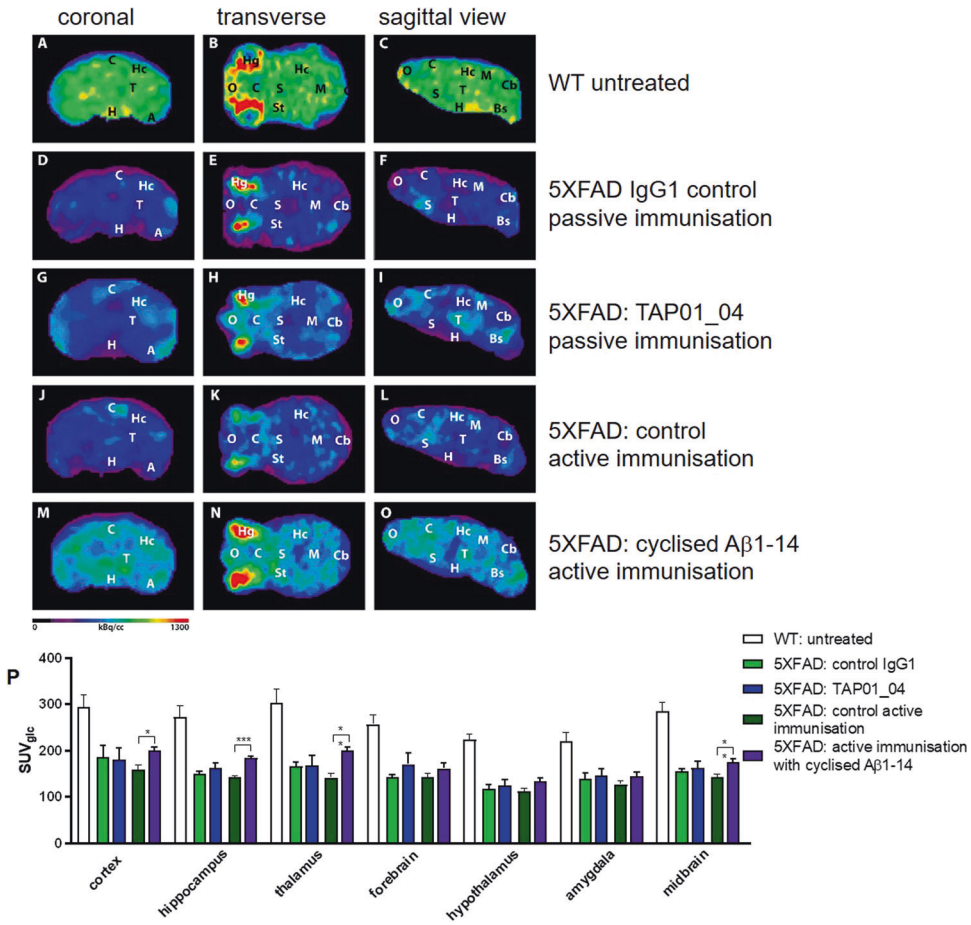

Fig. 3 Active immunisation of 5XFAD mice normalised brain glucose metabolism. ^{18}F-fluorodesoxyglucose-PET (^{18}F-FDG-PET) imaging to assess cerebral glucose metabolism in vivo, revealing a normalisation after active immunisation in 5XFAD. FDG-PET images (coronal, transverse and sagittal views) were obtained from untreated WT ($n = 4$) and active or passive immunised 5XFAD mice, with appropriate controls ($n = 5$ each group). **A**–**C** PET images of WT mice. **D**–**F** PET images of 5XFAD mice after control passive immunisation **G**–**I** PET images of 5XFAD mice after passive immunisation with TAP01_04. **J**–**L** PET images of 5XFAD mice following control active immunisation. **M**–**O** PET images of 5XFAD mice after active immunisation with the cyclised Aβ1-14 peptide. **P** Quantitative analysis of FDG-PET signal intensities of 5XFAD mice induced a substantial recovery of glucose metabolism in the cortex, hippocampus, thalamus and midbrain regions. Abbreviations: WT wild-type, A amygdala, Bs brain stem, C cortex, Cb cerebellum, H hypothalamus, Hc hippocampus, M midbrain, O olfactory bulb, S septum/basal forebrain, St striatum, T thalamus. Statistical analysis of the FDG-PET signal intensities was carried out by one-way ANOVA with Bonferroni multiple comparisons ($F = 11.11$, $p < 0.0001$, R squared 0.7024). The quantitative data are presented as mean ± S.E.M; $^{***}p < 0.001$; $^{**}p < 0.01$; $^{*}p < 0.05$.

no evidence of a beneficial effect on synapses was reported [39]. To develop a vaccine against AD would still be a great relief for AD patients and other stakeholders in the field.

Our working hypothesis was to develop a vaccine against AD that has no preference for binding to full-length Aβ, because it represents a physiological product of APP processing and as such is continuously generated in healthy individuals [40]. Moreover, the vaccine should not bind aggregated amyloid-Aβ found in plaques due to the negative side effects it induced in some AD patients [38]. The vaccine should however preferentially bind to N-truncated AβpE3-42 and Aβ4-42, as these variants are highly toxic in vivo and in vitro [5, 9], are stabilised as low-molecular weight oligomers in solution [18] and are associated with AD pathology but not with normal APP processing [7].

In the current work, we identified a unique conformational structure within the N-terminal region of Aβ bound to the TAP01 family of antibodies through X-ray crystallography studies of Aβ. We then engineered a stable form of the N-terminal Aβ1-14 peptide, which mimics the conformational epitope recognised by the TAP01 antibody, and showed that this cyclised Aβ1-14 peptide has the same antibody-bound structure as the AβpE3-14 amyloid peptide. This novel conformation is not found in any other crystal structure that has been reported, including any of the clinical-stage antibodies targeting Aβ. The crystal structures of several humanised anti-Aβ antibodies have been published but none reveals recognition of the novel Aβ conformation seen bound to TAP01. Crenezumab [41] binds multiple forms of Aβ with higher affinity reported for aggregates and the crystal structure revealed a sequential epitope with some conformational requirements for recognition [42]. Bapineuzumab is a humanised form of the murine monoclonal antibody 3D6, which targets the N-terminal region of Aβ [43] and binds the N-terminus of monomeric Aβ in a helical conformation [44]. Solanezumab, the humanised version of murine 266 antibody [45], is directed against the mid-domain of the Aβ peptide and is reported to recognise only soluble monomeric, not fibrillar, Aβ. Previously, we demonstrated strong amyloid plaque staining for solanezumab, crenezumab and bapineuzumab, whereas TAP01 showed hardly any binding to AD brain tissue sections [46]. BAN2401 is the humanised IgG1 version of the mouse monoclonal antibody mAb158, which selectively binds to large, soluble Aβ protofibrils [47]. Donanemab [48], ProBioDrug 6-1-6 and ProBioDrug 24-2-3 [49] are humanised

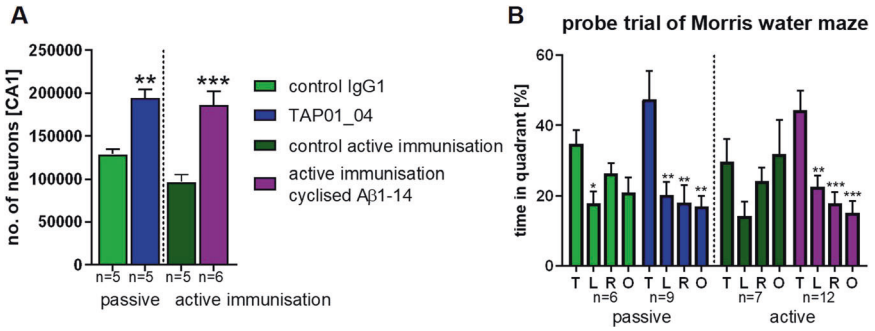

Fig. 4 Active and passive immunisation in Tg4-42 mice rescued on neuron number and on spatial reference memory. A The effect of active immunisation on neuron loss was assessed in the CA1 region of the hippocampus of immunised Tg4-42 mice and compared to effects of passive immunisation with TAP01_04 (passive immunisation: control IgG1 antibody; active immunisation: adjuvant without cyclic peptide). Active and passive immunisation rescued neuron loss, with no significant difference. One-way ANOVA ($p < 0.0001$; F = 16.23, R squared = 0.7413) followed by Bonferroni's multiple comparison test. **B** The effect of active and passive immunisation was assessed on spatial reference memory. Active and passive immunisation rescued spatial reference memory deficits, whereas control IgG1 antibody and adjuvant only as controls did not improve memory decline. One-way ANOVA was performed for each experimental group: TAP01_04 ($p < 0.001$, F = 7.523, R squared = 0.4136) and cyclised peptide ($p < 0.0001$, F = 10.93, R squared = 0.4271) followed by Bonferroni's multiple comparison test (p values shown are comparisons to target quadrant). T target quadrant, L left quadrant, R right quadrant, O opposite quadrant. Data presented as mean ± S.E.M; n = number of mice; ***$p < 0.001$; **$p < 0.01$; *$p < 0.05$.

versions of murine antibodies specific for N-terminal pyroglutamate derivatives of Aβ3-X.

Our binding studies indicate that while these other antibodies can bind to AβpE3-42, only TAP01 and the vaccine against cyclic Aβ1-14 binds to this novel conformation pseudo β-hairpin epitope, underpinning its unique properties and potential as a new treatments for AD. Active immunisation of preclinical AD mouse models with the cyclised Aβ1-14 vaccine reduced plaque load, rescued glucose metabolism, rescued memory deficits and rescued neuron loss.

Hardy and Allsop [50] suggested that the pathological cascade starts with deposition of amyloid-β, followed by tau phosphorylation and tangle formation, which leads to neuronal death. Later the amyloid hypothesis was further refined by a plethora of reports discussing the role of soluble amyloid oligomers rather than aggregated plaques in neuron and synaptic dysfunction leading to neuron loss typical for AD [1, 11, 16]. Moreover, the recent meta-analysis of pooled results from the 14 randomised controlled trials by Ackley et al. [51] found no correlation between the cognitive score and the small amyloid-plaque reduction in these studies. Portelius et al. [7] reported that dominating Aβ isoforms in different brain regions analysed from control, sporadic AD, and familial AD are Aβ1-42, AβpE3-42, Aβ4-42 and Aβ1-40. The authors showed that the relative importance of N-truncated isoforms of Aβ in comparison to full-length Aβ is a valuable tool to better understand the pathogenesis of AD [7]. It would therefore be of interest to assess the relative abundance of the TAPAS epitope in brain tissue and cerebrospinal fluid from patients with mild cognitive impairment, early and advanced AD pathology as well as plaque-negative non-AD and healthy control specimen. Mintun et al. [52] convincingly demonstrated that donanemab targeting plaque associated AβpE3-X is sufficient to achieve clinical meaningful therapy effects in early AD patients. This clinical trial is the first to show that AβpE3-42 is a relevant drug target to fight AD. Our current report is well in line with this assumption. We have identified a novel epitope, which mimics the N-terminus of pyroglutamate Aβ in its monomeric form. We do believe that it will have improved therapy effects, as neither the vaccine nor TAP01 antibodies preferentially react with amyloid plaques. We have demonstrated that stabilising the N-terminus of Aβ by using cyclic Aβ1-14 as a vaccine is crucial to induce a specific immune response targeting the TAPAS epitope. In contrast, capturing the normal unstabilised N-terminus of Aβ by passive immunisation with bapineuzumab or vaccination with full-length Aβ1-42 has not been successful in clinical trials.

In conclusion, we have developed a novel AD vaccine with unique features not related to any other vaccine or antibody in clinical development. The TAPAS family antibodies are uniquely positioned as the antibodies selectively target the early toxic N-terminal truncated species of Aβ found in abundance throughout the brains of AD patients. Moreover, the TAP01 antibody – and its humanised versions – are less likely to become trapped inside plaques thereby increasing the bioavailability after passive immunisation. This decreases the potential for the dose-limiting side effects that have so far proved problematic in clinical trials of other Aβ antibodies. The novel TAPAS family of antibodies have revealed two new attractive options for therapeutic intervention in AD, with either active immunisation using a cyclised peptide based vaccine, or treatment with a humanised TAP01 family therapeutic antibody (passive immunisation). The lead therapeutic antibody for clinical assessment is TAP01_04, which is a humanised variant of TAP01 retaining the high specificity and affinity of the mouse parent antibody [10, 35]. The optimum antibody format, such as full-length or Fab fragment, safety, tolerability and efficacy of TAP01_04 will now need to be evaluated in carefully planned human clinical trials. For a trail blazing vaccine-based approach to AD, formulation of the candidate cyclised Aβ peptides is likely to be a key factor to ensure a strong immune response and will require expertise from specialist vaccine development organisations. The design of the TRAILBLAZER-ALZ phase II registration quality trial to evaluate safety, tolerability and efficacy of donanemab [52] will be helpful to design clinical trials targeting the TAPAS epitope. In TRAILBLAZER-ALZ early AD patients were recruited based on a medium tangle load using Tau-PET imaging. As donanemab completely cleared plaques in two-thirds of participants and slowed cognitive decline in some patients, the pathological status appears crucial for a successful treatment strategy. The positive therapeutic outcomes from active immunisation with cyclic Aβ1-14 as well as the passive immunisation with the clinical lead candidate antibody suggest the potential for a vaccine to protect future generations from this terrible disease.

REFERENCES

1. McLean CA, Cherny RA, Fraser FW, Fuller SJ, Smith MJ, Beyreuther K, et al. Soluble pool of Abeta amyloid as a determinant of severity of neurodegeneration in Alzheimer's disease. Ann Neurol. 1999;46:860–6.
2. Shankar GM, Li S, Mehta TH, Garcia-Munoz A, Shepardson NE, Smith I, et al. Amyloid-beta protein dimers isolated directly from Alzheimer's brains impair synaptic plasticity and memory. Nat Med. 2008;14:837–42.

3. Walsh DM, Klyubin I, Fadeeva JV, Cullen WK, Anwyl R, Wolfe MS, et al. Naturally secreted oligomers of amyloid beta protein potently inhibit hippocampal long-term potentiation in vivo. Nature. 2002;416:535–9.
4. Shankar GM, Bloodgood BL, Townsend M, Walsh DM, Selkoe DJ, Sabatini BL. Natural Oligomers of the Alzheimer Amyloid-{beta} protein induce reversible synapse loss by modulating an NMDA-type glutamate receptor-dependent signaling pathway. J Neurosci.2007;27:2866–75.
5. Bayer TA, Wirths O. Focusing the amyloid cascade hypothesis on N-truncated Abeta peptides as drug targets against Alzheimer's disease. Acta Neuropathol. 2014;127:787–801.
6. Dunys J, Valverde A, Checler F. Are N- and C-terminally truncated Abeta species key pathological triggers in Alzheimer's disease? J Biol Chem.2018; 293:15419–28.
7. Portelius E, Bogdanovic N, Gustavsson MK, Volkmann I, Brinkmalm G, Zetterberg H, et al. Mass spectrometric characterization of brain amyloid beta isoform signatures in familial and sporadic Alzheimer's disease. Acta Neuropathol. 2010;120:185–93.
8. Grochowska KM, Yuanxiang P, Bar J, Raman R, Brugal G, Sahu G, et al. Post-translational modification impact on the mechanism by which amyloid-beta induces synaptic dysfunction. EMBO Rep. 2017;18:962–81.
9. Jawhar S, Wirths O, Bayer TA. Pyroglutamate Abeta - a hatchet man in Alzheimer disease. J Biol Chem.2011;286:38825–32.
10. Antonios G, Borgers H, Richard BC, Brauss A, Meissner J, Weggen S, et al. Alzheimer therapy with an antibody against N-terminal Abeta 4-X and pyroglutamate Abeta 3-X. Sci Rep. 2015;5:17338.
11. Haass C, Selkoe DJ. Soluble protein oligomers in neurodegeneration: lessons from the Alzheimer's amyloid beta-peptide. Nat Rev Mol Cell Biol. 2007;8:101–12.
12. Walsh DM, Selkoe DJ. Abeta oligomers - a decade of discovery. J Neurochem.2007;101:1172–84.
13. Kirkitadze MD, Bitan G, Teplow DB. Paradigm shifts in Alzheimer's disease and other neurodegenerative disorders: the emerging role of oligomeric assemblies. J Neurosci Res.2002;69:567–77.
14. Ono K, Condron MM, Teplow DB. Structure–neurotoxicity relationships of amyloid β-protein oligomers. Proc Natl Acad Sci. 2009;106:14745–50.
15. Chimon S, Shaibat MA, Jones CR, Calero DC, Aizezi B, Ishii Y. Evidence of fibril-like beta-sheet structures in a neurotoxic amyloid intermediate of Alzheimer's beta-amyloid. Nat Struct Mol Biol. 2007;14:1157–64.
16. Kayed R, Head E, Thompson JL, McIntire TM, Milton SC, Cotman CW, et al. Common structure of soluble amyloid oligomers implies common mechanism of pathogenesis. Science. 2003;300:486–9.
17. Oakley H, Cole SL, Logan S, Maus E, Shao P, Craft J, et al. Intraneuronal beta-amyloid aggregates, neurodegeneration, and neuron loss in transgenic mice with five familial Alzheimer's disease mutations: potential factors in amyloid plaque formation. J Neurosci.2006;26:10129–40.
18. Bouter Y, Dietrich K, Wittnam JL, Rezaei-Ghaleh N, Pillot T, Papot-Couturier S, et al. N-truncated amyloid beta (Abeta) 4-42 forms stable aggregates and induces acute and long-lasting behavioral deficits. Acta Neuropathol. 2013;126:189–205.
19. Kabsch W. Xds. Acta Crystallogr D Biol Crystallogr. 2010;66:125–32.
20. Winn MD, Ballard CC, Cowtan KD, Dodson EJ, Emsley P, Evans PR, et al. Overview of the CCP4 suite and current developments. Acta Crystallogr D Biol Crystallogr. 2011;67:235–42.
21. McCoy AJ, Grosse-Kunstleve RW, Storoni LC, Read RJ. Likelihood-enhanced fast translation functions. Acta Crystallogr D Biol Crystallogr. 2005;61:458–64.
22. Waterhouse A, Bertoni M, Bienert S, Studer G, Tauriello G, Gumienny R, et al. SWISS-MODEL: homology modelling of protein structures and complexes. Nucleic Acids Res. 2018;46:W296–303.
23. Emsley P, Cowtan K. Coot: model-building tools for molecular graphics. Acta Crystallogr D Biol Crystallogr. 2004;60:2126–32.
24. Murshudov GN, Vagin AA, Dodson EJ. Refinement of macromolecular structures by the maximum-likelihood method. Acta Crystallogr D Biol Crystallogr. 1997;53:240–55.
25. Liebschner D, Afonine PV, Baker ML, Bunkoczi G, Chen VB, Croll TI, et al. Macromolecular structure determination using X-rays, neutrons and electrons: recent developments in Phenix. Acta Crystallogr D Struct Biol. 2019;75:861–77.
26. Joosten RP, Salzemann J, Bloch V, Stockinger H, Berglund AC, Blanchet C, et al. PDB_REDO: automated re-refinement of X-ray structure models in the PDB. J Appl Crystallogr.2009;42:376–84.
27. Wittnam JL, Portelius E, Zetterberg H, Gustavsson MK, Schilling S, Koch B, et al. Pyroglutamate amyloid β (Aβ) aggravates behavioral deficits in transgenic amyloid mouse model for Alzheimer disease. J Biol Chem.2012;287:8154–62.
28. Jawhar S, Trawicka A, Jenneckens C, Bayer TA, Wirths O. Motor deficits, neuron loss, and reduced anxiety coinciding with axonal degeneration and intraneuronal Abeta aggregation in the 5XFAD mouse model of Alzheimer's disease. Neurobiol Aging. 2012;33:196.e129–40.
29. Wirths O, Bethge T, Marcello A, Harmeier A, Jawhar S, Lucassen PJ, et al. Pyroglutamate Abeta pathology in APP/PS1KI mice, sporadic and familial Alzheimer's disease cases. J Neural Transm (Vienna). 2010;117:85–96.
30. Morris R. Developments of a water-maze procedure for studying spatial learning in the rat. J Neurosci Methods.1984;11:47–60.
31. Bouter C, Henniges P, Franke TN, Irwin C, Sahlmann CO, Sichler ME, et al. F-FDG-PET detects drastic changes in brain metabolism in the Tg4-42 model of Alzheimer's Disease. Front Aging Neurosci. 2018;10:425.
32. Rominger A, Brendel M, Burgold S, Keppler K, Baumann K, Xiong G, et al. Longitudinal assessment of cerebral beta-amyloid deposition in mice overexpressing Swedish mutant beta-amyloid precursor protein using 18F-florbetaben PET. J Nucl Med.2013;54:1127–34.
33. Bouter C, Bouter Y. (18)F-FDG-PET in Mouse Models of Alzheimer's Disease. Front Med (Lausanne). 2019;6:71.
34. Chetelat G, Arbizu J, Barthel H, Garibotto V, Law I, Morbelli S, et al. Amyloid-PET and (18)F-FDG-PET in the diagnostic investigation of Alzheimer's disease and other dementias. Lancet Neurol. 2020;19:951–62.
35. Antonios G, Saiepour N, Bouter Y, Richard BC, Paetau A, Verkkoniemi-Ahola A, et al. N-truncated Abeta starting with position four: early intraneuronal accumulation and rescue of toxicity using NT4X-167, a novel monoclonal antibody. Acta Neuropathol Commun. 2013;1:56.
36. Schenk D, Barbour R, Dunn W, Gordon G, Grajeda H, Guido T, et al. Immunization with amyloid-beta attenuates Alzheimer-disease-like pathology in the PDAPP mouse. Nature. 1999;400:173–7.
37. Bayer AJ, Bullock R, Jones RW, Wilkinson D, Paterson KR, Jenkins L, et al. Evaluation of the safety and immunogenicity of synthetic Abeta42 (AN1792) in patients with AD. Neurology. 2005;64:94–101.
38. Gilman S, Koller M, Black RS, Jenkins L, Griffith SG, Fox NC, et al. Clinical effects of A{beta} immunization (AN1792) in patients with AD in an interrupted trial. Neurology. 2005;64:1553–62.
39. Holmes C, Boche D, Wilkinson D, Yadegarfar G, Hopkins V, Bayer A, et al. Long-term effects of Aβ42 immunisation in Alzheimer's disease: follow-up of a randomised, placebo-controlled phase I trial. Lancet. 2008;372:216–23.
40. Haass C, Hung AY, Schlossmacher MG, Oltersdorf T, Teplow DB, Selkoe DJ. Normal cellular processing of the beta-amyloid precursor protein results in the secretion of the amyloid beta peptide and related molecules. Ann N. Y Acad Sci. 1993;695:109–16.
41. Adolfsson O, Pihlgren M, Toni N, Varisco Y, Buccarello AL, Antoniello K, et al. An effector-reduced anti-beta-amyloid (Abeta) antibody with unique abeta binding properties promotes neuroprotection and glial engulfment of Abeta. J Neurosci.2012;32:9677–89.
42. Ultsch M, Li B, Maurer T, Mathieu M, Adolfsson O, Muhs A, et al. Structure of crenezumab complex with abeta shows loss of beta-hairpin. Sci Rep. 2016;6:39374.
43. Salloway S, Sperling R, Gilman S, Fox NC, Blennow K, Raskind M, et al. A phase 2 multiple ascending dose trial of bapineuzumab in mild to moderate Alzheimer disease. Neurology. 2009;73:2061–70.
44. Miles LA, Crespi GA, Doughty L, Parker MW. Bapineuzumab captures the N-terminus of the Alzheimer's disease amyloid-beta peptide in a helical conformation. Sci Rep. 2013;3:1302.
45. Dodart JC, Bales KR, Gannon KS, Greene SJ, DeMattos RB, Mathis C, et al. Immunization reverses memory deficits without reducing brain Abeta burden in Alzheimer's disease model. Nat Neurosci. 2002;5:452–7.
46. Bouter Y, Lopez Noguerola JS, Tucholla P, Crespi GA, Parker MW, Wiltfang J, et al. Abeta targets of the biosimilar antibodies of Bapineuzumab, Crenezumab, Solanezumab in comparison to an antibody against N-truncated Abeta in sporadic Alzheimer disease cases and mouse models. Acta Neuropathol. 2015;130:713–29.
47. Tucker S, Moller C, Tegerstedt K, Lord A, Laudon H, Sjodahl J, et al. The murine version of BAN2401 (mAb158) selectively reduces amyloid-beta protofibrils in brain and cerebrospinal fluid of tg-ArcSwe mice. J Alzheimers Dis.2015;43:575–88.
48. Dematttos RB, Lu J, Tang Y, Racke MM, Delong CA, Tzaferis JA, et al. A plaque-specific antibody clears existing beta-amyloid plaques in Alzheimer's disease mice. Neuron. 2012;76:908–20.
49. Piechotta A, Parthier C, Kleinschmidt M, Gnoth K, Pillot T, Lues I, et al. Structural and functional analyses of pyroglutamate-amyloid-beta-specific antibodies as a basis for Alzheimer immunotherapy. J Biol Chem.2017;292:12713–24.
50. Hardy J, Allsop D. Amyloid deposition as the central event in the aetiology of Alzheimer's disease. Trends Pharm Sci. 1991;12:383–8.
51. Ackley SF, Zimmerman SC, Brenowitz WD, Tchetgen Tchetgen EJ, Gold AL, Manly JJ, et al. Effect of reductions in amyloid levels on cognitive change in randomized trials: instrumental variable meta-analysis. BMJ. 2021;372:n156.
52. Mintun MA, Lo AC, Duggan Evans C, Wessels AM, Ardayfio PA, Andersen SW, et al. Donanemab in early Alzheimer's Disease. N. Engl J Med.2021;384:1691–704.

ACKNOWLEDGEMENTS

We thank Helen Payne for performing the ELISA for screening the sera from the 5XFAD mice and the protein production team at LifeArc for the generation of recombinant antibody material for in vivo studies. We thank Max Ueberück for performing immunostaining and plaque load analysis. This study was supported by a structural biology research partnership between LifeArc and Prof. Carr's group at the University of Leicester.

AUTHOR CONTRIBUTIONS

Conceptualisation: MDC, PB, TAB, DM. Methodology: CM, GH, MDC, PB, RC, EL, HP, JP, SD, CB, NB, YB. Investigation: GH, MDC, DM, PB, YB, TAB. Visualisation: GH, MDC, PB, TAB. Project administration: DM, PB. Supervision: GH, MDC, DM, PB, TAB. Writing – original draft: GH, MDC, PB, TAB. Writing – review & editing: GH, MDC, PB, TAB.

FUNDING

German Research Foundation grant INST 335/454-1 FUGG (NB).

COMPETING INTERESTS

LifeArc and University Medicine Goettingen hold patents on the project.

ADDITIONAL INFORMATION

Supplementary information The online version contains supplementary material available at https://doi.org/10.1038/s41380-021-01385-7.

Correspondence and requests for materials should be addressed to Preeti Bakrania, Mark D. Carr or Thomas A. Bayer.